RSC Advances

PAPER

View Article Online
View Journal | View Issue

Cite this: *RSC Adv.*, 2016, **6**, 49348

Hydroxylated di- and tri-styrylbenzenes, a new class of antiplasmodial agents: discovery and mechanism of action†

Naina Sharma,[ab] Dinesh Mohanakrishnan,[c] Amit Shard,[a] Abhishek Sharma,[ab] Arun K. Sinha‡*[a] and Dinkar Sahal*[c]

Received 7th March 2016
Accepted 27th April 2016

DOI: 10.1039/c6ra06059e

www.rsc.org/advances

The first systematic evaluation of the antiplasmodial activity of the hydroxystilbene family of natural products and di/tristyrylbenzenes is described. A library of **27** diversely substituted hydroxy stilbenoids was rapidly synthesized using modified Knoevenagel–Perkin-decarboxylation–Heck sequences from readily available starting materials (*i.e.* hydroxybenzaldehyde–phenylacetic acid–arylhalide). These compounds were evaluated for *in vitro* antiplasmodial activity against three different strains of *Plasmodium falciparum*. Notably, 4,4′4″-((1*E*,1′*E*,1″*E*)-benzene-1,3,5-triyltris(ethene-2,1-diyl))tris(2,6-dimethoxyphenol) (**27**), an octupolar stilbenoid, showed IC_{50} (μM) values of 0.6, 0.5 and 1.36 while a distyrylbenzene (**11**) showed IC_{50} values of 0.9, 2.0 and 2.7 against 3D7 (chloroquine sensitive), Dd2 and Indo (chloroquine resistant) strains of *Plasmodium falciparum* respectively. Moreover, **27** and **11**, which exhibited selectivity indices of 40 and >111 were also found to be nontoxic to the HeLa cell line. Microscopic studies revealed that the rings and trophozoites obtained from the **27** and **11** (an octupolar tristyrylbenzene and distyrylbenzene respectively) treated cultures were growth inhibited and morphologically deformed. These cultures also showed DNA fragmentation and loss of mitochondrial membrane potential ($\Delta\Psi_m$), suggestive of apoptotic death of the parasite. Together, these studies introduce di/tristyrylbenzenes as a new class of antimalarial agents.

Introduction

Malaria is one of the most infectious diseases known to mankind and it causes enormous mortality.[1] Although diverse, potent antimalarial agents including quinoline (*e.g. chloroquine*) and *endoperoxides* (*e.g. artemisinin*) are available, resistance against antimalarial drugs has been increasing at an alarming pace. Thus, the search for newer efficacious drugs as well as new molecular scaffolds possessing antimalarial activity remains a vital goal towards achieving control over malaria.[2]

Hydroxylated stilbenes represent an important class of natural products having special therapeutic significance owing to their various pharmacological activities[3] including anticancer and anti-inflammatory effects. Although there are few reports describing the antimalarial potential of natural prenylated,[4] glycosidic[5] or benzamide[6] containing stilbene derivatives (Fig. 1), however, the exploration of higher order stilbenoids (dimeric/trimeric) against *P. falciparum* has not received much attention. For instance, although distyrylbenzenes (DSBs) find important applications in the detection[7] and treatment[8] of neurodegenerative disease, to date DSBs as well as tristyrylbenzene have never been investigated as antimalarials.

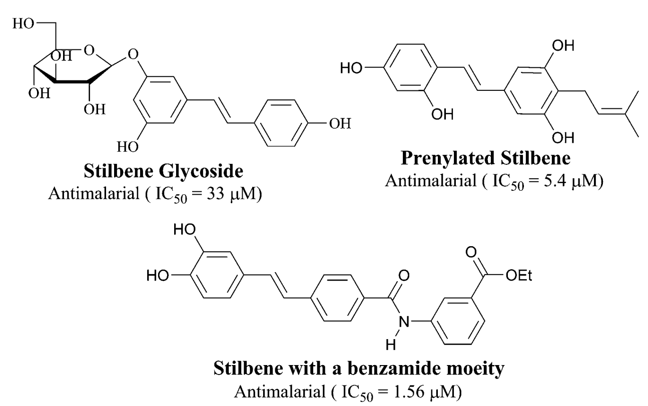

Fig. 1 Example of some previously reported antimalarial stilbenoids.

[a]Natural Plant Products Division, CSIR-Institute of Himalaya Bioresource Technology, Palampur, H.P.-176061, India. E-mail: aksinha08@rediffmail.com

[b]Department of Chemistry, University of Illinois at Urbana-Champaign, Urbana, Illinois 61801, USA

[c]Malaria Drug Discovery Group, International Centre for Genetic Engineering and Biotechnology, Aruna Asaf Ali Marg, New Delhi 110067, India. E-mail: dinkar@icgeb.res.in

† Electronic supplementary information (ESI) available: ^{1}H NMR, ^{13}C NMR data of selected compounds. See DOI: 10.1039/c6ra06059e

‡ Present address: Medicinal and Process Chemistry, C.S.I.R-Central Drug Research institute (C.D.R.I.), Lucknow 226031, India, Email: ak.sinha@cdri.res.in

Pursuant to our interest in synthesis[9–11] and biological activities[12] of hydroxylated stilbenoids it was envisaged to synthesize a library of monomeric, dimeric and trimeric hydroxylated stilbenoids and screen them as antimalarials. Herein we show that hydroxylated octupolar[13] stilbenoid (**27**) and a distyrylbenzene (**11**) are highly potent antiplasmodial agents across chloroquine sensitive and chloroquine resistant strains of *P. falciparum*. Mechanistic studies have indicated that these molecules cause morphological deformations, DNA fragmentation and loss of mitochondrial membrane potential ($\Delta\Psi_m$) in malaria parasite suggesting apoptotic cell death.

Results and discussion

Synthesis of hydroxylated stilbenoids

Amongst the various possible synthetic routes towards hydroxystilbenoids (A–HC=CH–B), the modified Knoevenagel Heck[9] and Perkin[10] approaches were utilized, as these allowed a rapid access to diversely functionalized stilbenoids using readily available starting materials such as hydroxylated benzaldehyde, phenyl acetic acid and halobenzene. A library comprising of 27 diversely substituted hydroxylated stilbenoids including stilbenes, distyrylbenzenes and tristyrylbenzenes was synthesized. Thus, hydroxylated stilbenes, **1** to **8** (Scheme 1) were obtained *via* synthesis of hydroxy substituted styrenes (ring **A**) using modified Knoevenagel Doebner-decarboxylation approach followed by their *in situ* Heck coupling[9] with diversely substituted aryl halides (ring **B**).

On the other hand, **9** & **10** possessing bromo functional group on ring **B** (Scheme 1) were synthesized *via* modified Perkin condensation–decarboxylation[10] reaction. Hydroxy substituted symmetrical DSBs (**11–19**) with different substitution patterns on rings **A** and **B** (**11–17**) or with variations on ring **C** (**18** & **19**) were synthesized *via* sequential Knoevenagel/decarboxylation–double Heck reaction in one-pot.[9]

Unsymmetrical DSBs **20–26** (Scheme 1) having a 4-hydroxy substitution at ring **B** and different electron releasing groups at ring **A**, were synthesized by Perkin–Knoevenagel-condensation–decarboxylation–Heck strategy under microwave irradiation.[11]

In the course of our efforts to further enhance the diversity of our panel of higher order stilbenoids, the oligophenylenevinylene (OPV, **27**)[9] with 4-hydroxy-3,5-dimethoxy substitution (Scheme 1) was prepared *via* Heck reaction of *in situ* formed 4-hydroxy-3,5-dimethoxystyrene with 1,3,5-tribromobenzene in DMF under reflux conditions. In order to gauge the specific effect of octupolar moiety, an analogue[14] of **27** possessing biaryl linkage (**28**, Scheme 2) was synthesized *via* palladium catalyzed triple Suzuki coupling of 1,3,5-tribromobenzene with 3,4,5-trimethoxy-phenylboronic acid under microwave in the presence of $Pd(PPh_3)_4$, K_2CO_3 in dioxane : water (5 : 1).

Biological activity of monomeric/dimeric/trimeric stilbenes

The hydroxylated (**1–8**) and brominated (**9–10**) stilbenes were subjected to microtiter plate high-throughput format SYBR Green I fluorescence based antiplasmodial screen.[15] As shown in Table 1, 4,4′-dihydroxystilbene (**1**) displayed an IC_{50} of 92 μM against the 3D7 strain of *P. falciparum*. Replacement of one of the hydroxy groups with methoxy *i.e.* 4-hydroxy-4′-methoxystilbene (**2**) caused a decrease in potency (IC_{50} > 100 μM).

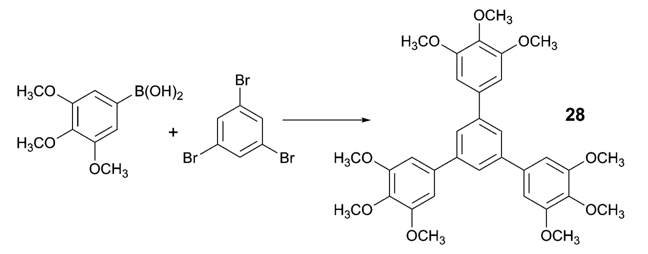

Scheme 2 General conditions: 3,4,5-trimethoxyphenylboronic acid, 1,3,5-tribromobenzene, K_2CO_3, $Pd(PPh_3)_4$, MW (250 W, 115 °C) in dioxane : water (5 : 1) for 35 min.

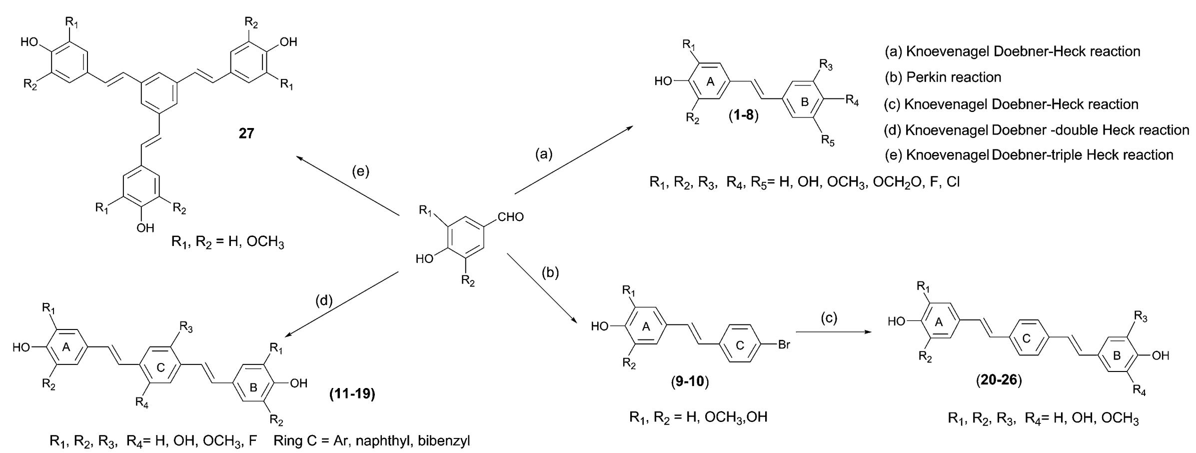

Scheme 1 Reagents and conditions: (a) substituted iodobenzene, $CH_2(COOH)_2$, $Pd(PPh_3)_4$, piperidine, LiCl, DMF, reflux 10 h (b) *p*-bromophenylacetic acid, *N*-methylimidazole, piperidine, PEG-200, microwave (160 °C) for 25 min (c) malonic acid, substituted *p*-hydroxybenzaldehyde, $Pd(PPh_3)_4$, piperidine, LiCl, DMF, MW (150 °C) for 45 min (d and e) $CH_2(COOH)_2$, piperidine, $Pd(PPh_3)_4$, LiCl, substituted 1,4-diiodobenzene in condition (d) and 1,3,5-tribromobenzene in condition (e) were refluxed in DMF for **14**.

Table 1 Antiplasmodial activities of unsymmetrical and symmetrical stilbenoids against *P. falciparum* 3D7 strain

Compound no.	Structure	IC_{50} (μM)
1	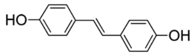	92
2	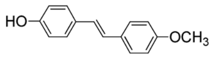	>100
3	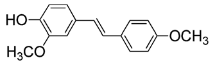	>50
4	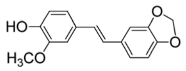	>100
5	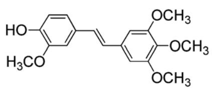	47.5
6	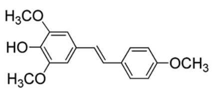	>50
7	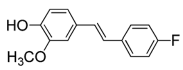	>100
8	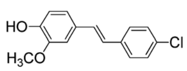	88
9	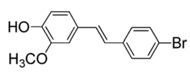	99
10	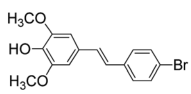	63
11	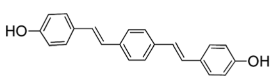	0.9
12	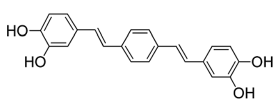	66
13	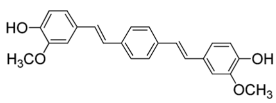	18
14	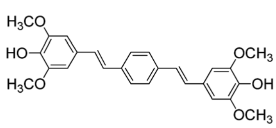	11
15	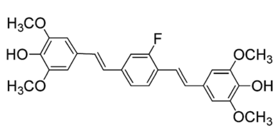	50
16	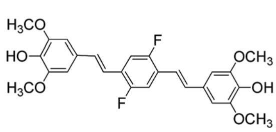	26
17	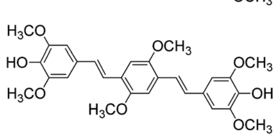	15
18	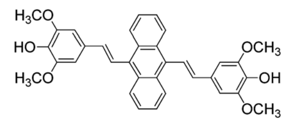	16
19	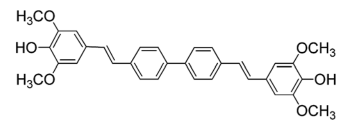	>100
20	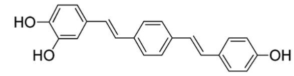	>100
21	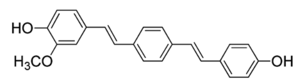	1.9
22	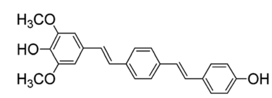	2.4
23	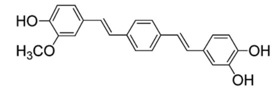	6.0
24	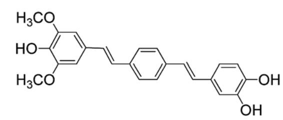	1.4
25	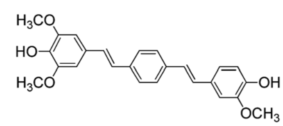	15.0
26	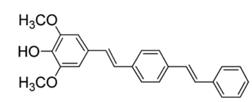	>100
27	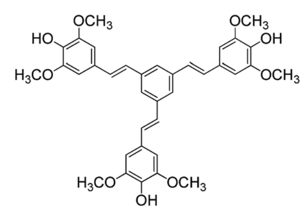	0.62
28	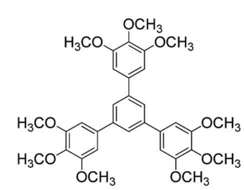	>100
Chloroquine		40 nM

Later on, 4-hydroxy-3-methoxy substitution on ring **A** was kept constant and the effects of different electron releasing (Table 1, **3–5**) and electron withdrawing groups (**7–9**) on the ring **B** were evaluated. Interestingly, **5** (IC_{50} 47.5 μM) possessing greater electron density on both rings showed slightly better antiplasmodial activity than **1–4** and **7–9** (IC_{50} > 50 μM). However none of these monomeric stilbenoids showed significant antimalarial potential.

Hence, it was decided to extend the conjugation of the core stilbene monomers (Table 1, **1–10**) and evaluate the antiplasmodial potency of resulting distyrylbenzenes (**11**). It is evident from the screening results that a dimer of the inactive 4,4′-dihydroxy monomeric stilbene (**1**, IC_{50} 92 μM) *i.e.* 4,4′-dihydroxy substituted symmetrical distyrylbenzene (**11**) displayed promising activity (IC_{50} 0.9 μM) against the 3D7 strain of *P. falciparum*. An increase in hydroxy substitution on rings **A** and **B** of dimeric stilbene led to decreased antiplasmodial potential (**12**, IC_{50} 66.0 μM) while introduction of methoxy substitution (**13**) resulted in comparatively better activity (IC_{50}18 μM) than **12**. Interestingly, a further increase in electron density (**14**) slightly improved the activity (IC_{50} 11 μM). On the other hand dimeric stilbenes **15** (IC_{50} 50 μM) and **16** (IC_{50} 26 μM) having the same substituents as **14**, but having the electron withdrawing fluoro groups on ring **C** (**15** & **16**) showed decrease in antiplasmodial potency. Further, the replacement of central ring **C** with 2,5-dimethoxybenzene (**17**) & anthracenyl (**18**) led to moderate antiplasmodial activity (**17**, IC_{50} 15 μM & **18**, IC_{50} 16 μM), whereas the presence of a biaryl ring (**19**) diminished the activity (IC_{50} > 100 μM). It is evident from above discussion that the presence of either 4-hydroxy or 4-hydroxy-3,5-dimethoxy substitution on terminal rings **A** & **C** augments antiplasmodial activity.

After the antiplasmodial analysis of the symmetrical DSBs (Table 1, **11–19**), it was decided to evaluate the effect of unsymmetrical substitution pattern of distyrylbenzenes (Table 1, **20–26**). The antiplasmodial evaluation results for the unsymmetrical DSBs (**20–26**) indicated that among the three compounds (**20–22**), the DSB possessing 3,4-dihydroxy functionality at ring **A** (**20**) (IC_{50} > 100 μM) was inactive (Table 1). Surprisingly, slight variation of substituents *i.e.* having 4-hydroxy-3-methoxy (**21**, IC_{50} 1.9 μM) and 4-hydroxy-3,5-dimethoxy (**22**, IC_{50} 2.4 μM) substitutions at ring **A**, significantly enhanced the antiplasmodial activity (Table 1).

Interestingly, a further increase in electron density on ring **B** (**23** & **24**) of dimeric stilbenes led to decreased activity in **23** (IC_{50} 6 μM) while increase in potency was observed in case of **24** (IC_{50} 1.4 μM). Further, replacement of a hydroxy group with methoxy in ring **B** (**25**) decreased the activity (IC_{50} 15 μM). Similarly, **26** (IC_{50} > 100 μM) having an unsubstituted ring **B** was also found to be inactive. In view of above results, potent activity seems to be associated with the presence of 4-hydroxy-3-methoxy (ring **A**) and 4-hydroxy (ring **B**) (**21**) or 4-hydroxy-3,5-dimethoxy *i.e.* syringol (ring **A**) and 3,4-dihydroxy (ring **B**) (**24**). Thereafter, the tristyrylbenzene **27** (Table 1) was also evaluated for antimalarial activity. Interestingly it was found to be the most potent *Pf*3D7 inhibitor with IC_{50} 0.62 μM. In contrast to octupolar stilbene (**27**, IC_{50} 0.62 μM), the triarylbenzene (**28**) with IC_{50} > 100 μM (Table 1, Scheme 2) was found to be inactive suggesting a specific role of tristyrylbenzene moiety in *P. falciparum* inhibition.

It is worthwhile to mention that unlike DSBs (**11–26**) which have been used for the detection/treatment of Alzheimer's disease, such octupolar stilbenoids (**27**) have not yet been explored as biologically active agents even though their application in material science[16] and non-linear optics[17] is well documented. The dose dependent growth inhibition of malarial parasites by potent stilbenoids is shown in Fig. 2A. Since test molecules can interfere with SYBR green fluorescence,[15] all the test molecules were checked for (a) auto fluorescence and (b) quenching effects in cultures of malaria parasites. Measurement of auto florescence helps avoid false negatives among the active molecules which may be fluorescent. Evaluation of quenching effects helps to avoid false negatives from test molecules that may be quenchers of fluorescence but may have no antiplasmodial action. As shown in Fig. 2B, none of the **27** molecules studied by us (a) had intrinsic fluorescence or (b) had the ability to quench the fluorescence due to SYBR Green. This gives validity to the results obtained by the SYBR Green assay. The results of SYBR Green assay were further corroborated by examining the time dependent effects of **11** & **27** on the malaria parasite using microscopy on Giemsa stained smears of parasite cultures (Fig. 3).

Subsequently, trimeric **27** (Table 1) and some potent DSBs (IC_{50} < 2.5 μM) (Table 1, **11**, **21**, **22** & **24**) were explored against two chloroquine resistant strains of *P. falciparum* (*Pf*Dd2 & *Pf*INDO) (Table 2). Importantly, **27** displayed a broad spectrum antiplasmodial potential with IC_{50} 1.36 μM (*Pf* INDO) and 0.5 μM (*Pf* Dd2). Further, **27** also showed a selectivity index of 40 against HeLa cell lines thereby indicating it to be non-toxic.

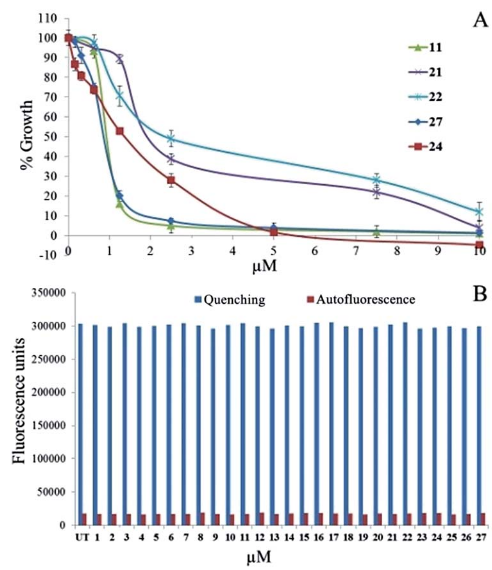

Fig. 2 (A) Dose dependent antiplasmodial activities of potent stilbenoids estimated by SYBR green assay against *P. falciparum* 3D7. Compound numbers and the corresponding color codes are indicated in the strip on the right. Standard deviation bars at each data point have been calculated from triplicate observations. (B) Data validation. Fluorescence intensity test of autofluorescent or quenching nature of test molecules: untreated (UT) or drug (**1–27**) treated cultures were subjected to fluorescence intensity measurements using excitation/emission of 480/535 nm (red bars). The nearly identical intensities across control and test samples indicate that the test compounds caused no interference due to autofluorescence. Control and test molecule treated cultures were read for fluorescence intensities following lysis by SYBR Green I containing lysis buffer (blue bars). The nearly identical intensities across control and test samples indicate absence of quenching effects.

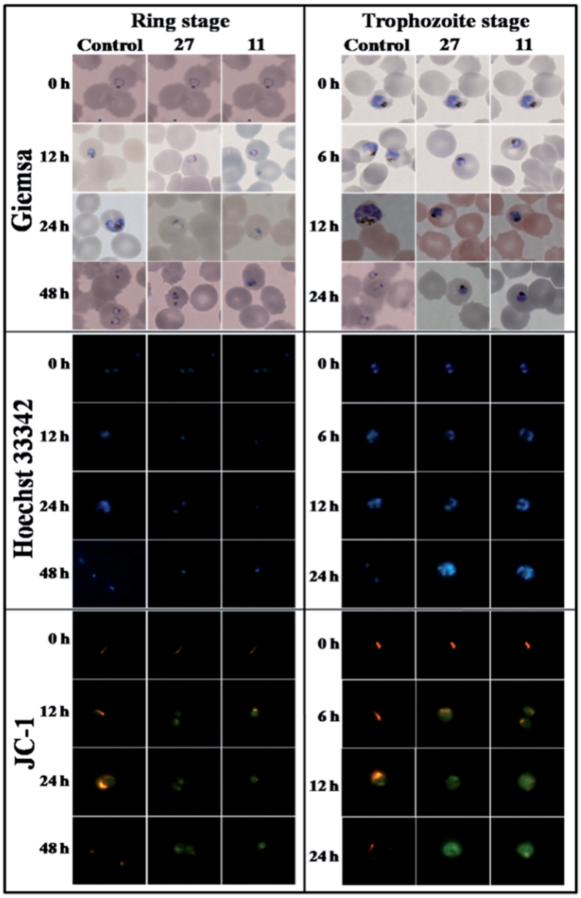

Fig. 3 Microscopic studies indicating apoptotic cell death in **11** and **27** treated malaria parasites. Ring and trophozoite stages of *Pf*3D7 were treated with compounds **27** and **11** at their IC_{90} values for different time points indicated against each panel. Giemsa staining showed stressed and shrunken "crisis forms" in **27** & **11** treated cultures. Drug treated ring and trophozoite stages lagged behind their respective controls in terms of ring to trophozoite and trophozoite to schizont transitions. Increased fluorescence of Hoechst 33342 in treated trophozoites (24 h) suggests DNA condensation and fragmentation in malaria parasites. JC-1 staining indicates loss of mitochondrial membrane potential in **27** and **11** treated ring and trophozoites stages. For zoom of these images please see ESI Fig. S1a–c.†

Probing the antiplasmodial action of DSB 11 and octupolar stilbenoid 27

Microscopic examination of **11** and **27** treated parasite cultures revealed stressed and shrunken "crisis forms" (Fig. 3). This led us to explore if these two lead compounds were triggering apoptotic programmed cell death in the parasite. Synchronized parasite cultures of *Pf*3D7 were incubated with **27** and **11** at their respective IC_{90} {1.3 μM (**27**) & 1.8 μM (**11**)} for 12, 24, 48 h (rings) and 6, 12, 24 h (trophozoites). In contrast to the healthy appearances of the untreated control cultures and their sequential transition to the subsequent stages, the pycnotic appearances of the rings and the trophozoites in the treated cultures suggested that stress and probable death had prevented the parasite to transit to the respective next stages of its life cycle. It may be noted that cell shrinkage (crisis form) which can be readily observed under the microscope, is one of the major characteristic features of apoptotic cell death.[18] The shrunken, condensed and darkly stained nuclei of **27** and **11** treated rings and trophozoites stages as observed by Giemsa staining (Fig. 3 and ESI Fig. S1a† for zoom) led us to look for other indicators of apoptotic cell death.

DNA fragmentation and condensation are among the major features of apoptosis.[18] Minor groove binding DNA stain, Hoechst 33342 was used to monitor DNA condensation in drug treated parasite cultures. As shown (Fig. 3), the control rings showed progressively greater staining as the rings matured to become early trophozoites (12 h) and late trophozoites (24 h). In contrast, **11** and **27** treated rings failed to become trophozoites and appeared as highly condensed dot like bodies till 48 h. Staining with Hoechst 33342 in control parasite cultures owes its low intensity to the fact that highly compact and condensed native chromatin exposes very few sites for the binding of dyes like the Hoechst 33342. DNA fragmentation results in higher degree of exposure and greater number of binding sites resulting in brighter fluorescence associated with cells undergoing apoptosis. The Hoechst 33342 staining of **11** and **27** treated trophozoites showed strong fluorescence at 12 h. At 24 h while the control culture showed dull staining in the form of small dots corresponding to rings, the treated cultures showed strong fluorescence originating from arrested trophozoites harboring fragmented chromatin spread over a large area (Fig. 3 and ESI Fig. S1b† for zoom). It is interesting to note that the chromatin fragmentation observed here bears resemblance to the pattern of chromatin fragmentation we have earlier observed in trophozoite stage cultures treated with stilbene–chalcone hybrids.[12] While Hoechst 33342 staining based results described above were suggestive of DNA fragmentation, a more direct proof of DNA fragmentation was obtained from agarose gel electrophoretic analysis of genomic DNA obtained from **11**/**27** treated *vs.* control parasite cultures (Fig. 4). While the untreated culture showed the only intense band of genomic

Table 2 Antiplasmodial potential, resistance and selectivity indices for potent stilbenoids

	SYBR green assay IC_{50} (μM)			Resistance index		Selectivity index	
Comp. no.	*Pf*3D7	*Pf*3D2	*Pf*Indo	IC_{50} Dd2/IC_{50} 3D7	IC_{50} Indo/IC_{50} 3D7	IC_{50} HeLa/IC_{50} 3D7	IC_{50} L929/IC_{50} 3D7
11	0.9	2.0	2.7	2.2	3	>111.11	>111.11
21	1.9	3.2	2.2	1.5	1.2	15.8	>52.6
22	2.4	3.2	2.8	1.3	1.2	4.7	>41.6
24	1.4	6.25	6.1	4.4	4.5	18.6	39.3
27	0.62	0.5	1.36	0.8	2.2	40.3	29.0

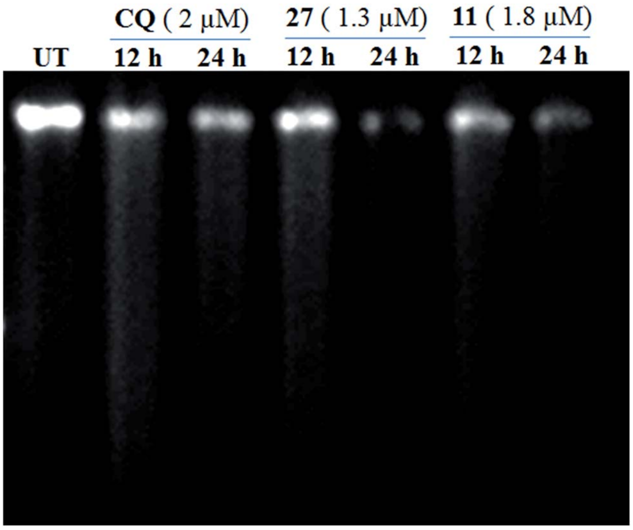

Fig. 4 Detection of DNA fragmentation in **11** and **27** treated *Pf*Indo by agarose gel electrophoresis: early trophozoite stage cultures were treated with indicated concentrations of CQ (+ control), **11** and **27** for 12 and 24 h. The DNA isolated from parasites was subjected to electrophoretic separation. Note the strong intensity of genomic DNA band in untreated (UT) culture. Drug treated cultures band intensities of genomic DNA is diminished with simultaneous appearance of low MW DNA fragments.

band, the DNA obtained from **11**/**27** treated cultures showed a diminished intensity of genomic DNA together with a streak of low molecular weight DNA fragments. Interestingly, the intensity of these fragmented pieces of genomic DNA was higher in cultures from 12 h exposure than from analogous cultures resulting from 24 h exposure to **11**/**27**. This data suggests that **11** and **27** may induce DNA fragmentation at times earlier than 12 h and 24 h may be the time corresponding to extensive DNA breakdown to sizes too small to be detected by this gel based staining method. Indeed this time dependent phenomenon observed with **11**/**27** found a good match with chloroquine (used as positive control in this experiment) which also showed a higher intensity of fragmented DNA bands at 12 h than at 24 h.

Loss of mitochondrial membrane potential ($\Delta\Psi_m$), a hallmark of apoptosis[19] was observed using JC-1 dye fluorescence microscopy in **27** and **11** treated malarial parasites. This dye is known to acquire a red color upon aggregation in the ambience of a high $\Delta\Psi_m$. When $\Delta\Psi_m$ is abolished by drugs that trigger apoptosis, the disaggregation of the dye causes its color to change from red to green. Ring stage parasites treated with **27** and **11** showed complete loss of $\Delta\Psi_m$ (fully green) at 12 h and 24 h respectively (Fig. 3 and ESI Fig. S1c† for zoom). However, the vulnerability of trophozoites to **11** and **27** appeared to be identical since 12 h treatments with each one of them resulted in complete loss of $\Delta\Psi_m$.

Apoptosis, a process of programmed cell death involving features of cell shrinkage, DNA fragmentation, chromatin condensation, formation of apoptotic bodies, translocation of phosphatidyl serine from inner to the outer leaflet of the plasma membrane and the loss of mitochondrial membrane potential has found vivid description in multicellular organisms.[20,21] However it is now becoming increasingly apparent that the evolutionary origins of apoptosis may go back to unicellular organisms like *Leishmania*, *Plasmodium*, yeast, bacteria, blastocystis, *Trypanosoma*, and *Trichomonas*.[22,23] Our observation of apoptotic death in stilbenoid treated *Plasmodium falciparum* represents a new avenue of targeting a sensitive niche of the malaria parasite with a new pharmacophore. The high selectivity with which **11** and **27** have been found to target the blood stage malaria parasite but not the mammalian cells like the HeLa and L929 suggests that the apoptotic machinery of *Plasmodium*, a primitive protozoan, may be characteristically different from the corresponding machinery in the highly evolved mammalian cells. It is worth noting that CQ has also been found to inflict apoptotic death in malaria parasite.[24,25] Moreover the report of a putative *P. falciparum* metacaspase (*Pf* MCA-1)[25,26] and apoptotic features in *P. berghei ookinetes*[27,28] endorse the presence of apoptotic machinery in the malaria parasite. Thus apoptosis machinery of the malaria parasite appears to be a valid target worthy of attack by novel pharmacophores like the stilbenoids in the present study.

Conclusions

In conclusion, the first systematic antiplasmodial evaluation of a library of hydroxy substituted monomeric and oligomeric stilbenoids (stilbenes, distyrylbenzenes and tristyrylbenzene) was conducted. Importantly, the above study led to the introduction of distyrylbenzenes and tristyrylbenzene as a novel class of potent antiplasmodial scaffolds. Compound **11**, a dimeric form of hydroxyl stilbene {IC_{50}: *Pf* 3D7 0.9 μM, *Pf*Dd2 2.0 μM, *Pf*Indo 2.7 μM, selectivity index > 111 (HeLa and L929)} remarkably shows high antiplasmodial potency and high selectivity index. Likewise, compound **27**: 4,4′4″-((1*E*,1′*E*,1″*E*)-benzene-1,3,5-triyltris(ethene-2,1-diyl))tris(2,6-dimethoxyphenol), displayed highly promising antiplasmodial activity (IC_{50}: *Pf* 3D7 0.62 μM, *Pf* Dd2 0.5 μM, *Pf* Indo 1.36 μM) as well as good selectivity indices of 40.3 (HeLa) and 29 (L929). Further mechanistic investigations have revealed that distyrylbenzene (**11**) and octupolar stilbenoid (**27**) trigger selective apoptotic cell death in malaria parasite.

Experimental section

Materials & instruments

All the starting materials were reagent grade. The palladium catalyst was purchased from Aldrich and used as such. The substituted benzaldehydes, haloarenes, 4-bromophenylacetic acid and all other reagents were obtained from commercial sources (Merck and Aldrich). The solvents used for isolation/purification of compounds were obtained from commercial sources (Merck) and used without further purification. Column chromatography was performed using silica gel (Merck, 60–120 mesh size). The chromatographic solvents are mentioned as volume : volume ratios. ^{1}H (300 MHz) and ^{13}C (75.4 MHz) NMR spectra were recorded on a Bruker Avance-300 spectrometer. The following abbreviations have been used to designate chemical shift multiplicities: s = singlet, d = doublet, t =

triplet, m = multiplet. The ^{13}C NMR spectra are proton decoupled. The melting points were determined on a digital Barnsted Electrothermal 9100 apparatus and are uncorrected. HRMS-ESI spectra were determined using micromass Q-TOF ultima spectrometer and reported as *m*/*z* (relative intensity). A CEM Discover® focused microwave oven (2450 MHz, 300 W) was used for reactions.

Representative procedure for the synthesis of (*E*)-4,4′-(ethene-1,2-diyl)diphenol (1) *via* Knoevenagel condensation–double decarboxylation–Heck coupling reaction (Table 1)

Malonic acid (0.64 g, 6.15 mmol) was taken in a round bottom flask and piperidine (0.45 mL, 4.6 mmol) added gradually. The above mixture was stirred in DMF (15 mL) for 2 min at room temperature. Thereafter, 4-hydroxybenzaldehyde (1a, 1.51 mmol), 4-iodophenol (0.2 g, 0.90 mmol), $Pd(PPh_3)_4$ (0.025 mmol), piperidine (3.1 mmol) and LiCl (0.07 mmol) were added, and the reaction mixture allowed to reflux for 10 h. The above mixture was cooled to room temperature and filtered through celite and washed with ethyl acetate. The filtrate was poured into water (100 mL, acidified with dil. HCl, pH = 5–6) and extracted with ethyl acetate (2 × 40 mL). The combined organic layer was washed with water (1 × 30 mL), brine (1 × 10 mL), dried over Na_2SO_4 and vacuum evaporated. The obtained residue was subsequently purified by column chromatography on silica gel (60–120 mesh size) using hexane : ethyl acetate (9.5 : 0.5) to give a solid which was further recrystallized in methanol to provide pure 4,4′-dihydroxystilbene (**1**, Table 1).

(*E*)-4,4′-(Ethene-1,2-diyl)diphenol (1).[29] White solid (33% yield), mp 200–202 °C, ^{1}H NMR δ (CD_3COCD_3, 300 MHz), 8.54 (2H, s), 7.39 (4H, d, J = 8.7 Hz), 6.96 (2H, s), 6.82 (4H, d, J = 8.7 Hz); ^{13}C NMR δ (75.4 MHz, CD_3COCD_3), 157.3, 129.9, 127.8, 125.9 and 115.9.

The same procedure was also followed for synthesis of other hydroxylated stilbenes including **2–8** (Table 1).

Representative procedure for the synthesis of (*E*)-4-(4-bromostyryl)-2-methoxyphenol (9, Table 1) *via* modified Perkin condensation–decarboxylation reaction

A stirred mixture of 4-bromophenylacetic acid (3.6 mmol), methylimidazole (4.9 mmol), piperidine (4.9 mmol) and 4-hydroxy-3-methoxybenzaldehyde (0.5 g, 3.28 mmol) in polyethylene glycol-200 (3–4 mL) was irradiated under focused monomode microwave (150 W, 160 °C) fitted with reflux condenser for 25 min. After the completion of reaction, the reaction mixture was cooled and acidified with dil. HCl (pH = 5). Then the aqueous layer was extracted with ethyl acetate (2 × 20 mL) and the organic layer was dried over sodium sulfate, vacuum distilled to obtain crude product which was further purified by column chromatography using silica-gel (60–120 mesh size) with a 0.5 : 9.5 mixture of ethyl acetate : hexane to give the pure stilbene (**9**).

(*E*)-4-(4-Bromostyryl)-2-methoxyphenol (9).[30] Cream solid (42% yield), mp 120–122 °C, ^{1}H NMR δ ($CDCl_3$, 300 MHz), 7.50 (2H, d, J = 8.5 Hz), 7.38 (2H, d, J = 8.5 Hz), 7.10–7.02 (3H, m), 6.95 (2H, d, J = 8.3 Hz), 5.75 (1H, s), 3.97 (3H, s); ^{13}C NMR δ (75.4 MHz, $CDCl_3$), 147.1, 146.2, 136.9, 132.1, 130.0, 129.7, 128.1, 125.6, 121.2, 121.0, 115.0, 108.6 and 56.3.

The above procedure was also followed for synthesis of 4-bromo-4′-hydroxy-3′,5′-dimethoxystilbene (**10**, Table 1).

Representative procedure for the synthesis of 4,4′-((1*E*,1′*E*)-1,4-phenylenebis(ethene-2,1-diyl))diphenol 11, *via* Knoevenagel condensation–double decarboxylation–double Heck coupling reaction (Table 1)

Malonic acid (21.6 mmol) was taken in a round bottom flask and piperidine (16.45 mmol) added gradually. The above mixture was stirred in DMF (25 mL), for 2 min at room temperature. Thereafter, 4-hydroxybenzaldehyde (2.7 mmol), 1,4-diiodobenzene (0.25 g, 0.755 mmol), $Pd(PPh_3)_4$ (0.045 mmol), piperidine (10.55 mmol) and LiCl (0.12 mmol) were added and the reaction mixture allowed to reflux for 14 h. The above mixture was cooled to room temperature and filtered through celite. The filtrate was poured into water (250 mL, acidified with dil. HCl, pH = 5) and extracted with ethyl acetate (3 × 50 mL). The combined organic layer was washed with water (1 × 50 mL), brine (1 × 20 mL), dried over Na_2SO_4 and vacuum evaporated. The resultant residue was subsequently purified by column chromatography on silica gel (60–120 mesh size) using hexane : ethyl acetate (6 : 4) and obtained solid was recrystallized with methanol to provide pure product (**11**).

4,4′-((1*E*,1′*E*)-1,4-Phenylenebis(ethene-2,1-diyl))diphenol (11).[31] Grey solid (61% yield), mp 362–366 °C (lit. mp 310–312 °C), ^{1}H NMR (DMSO, 300 MHz), δ (ppm) 9.68 (2H, s), 7.51–7.45 (8H, m), 7.13–7.04 (4H, m), 6.78 (4H, s); ^{13}C NMR (75.4 MHz, DMSO), δ (ppm) 157.7, 136.7, 128.6, 128.5, 128.3, 126.8, 125.3, 116.0.

The above procedure was also followed for synthesis of other symmetrical distyrylbenzenes **12–19** (Table 1).

Representative procedure for the synthesis of 4-((*E*)-4-((*E*)-4-hydroxystyryl)styryl)benzene-1,2-diol (20, Table 1) from 3,4-dihydroxy benzaldehyde

To a stirred mixture of 4-bromophenylacetic acid (1.5 g, 7.0 mmol), methylimidazole (0.46 mL, 5.8 mmol) and piperidine (0.62 mL, 6.30 mmol) in PEG-200 (5 mL), 3,4-dihydroxybenzaldehyde (3.94 mmol) was added and the reaction mixture irradiated under microwave (180 W, 150 °C) for 20 min. Thereafter, a mixture of malonic acid (4.08 g, 39.2 mmol), piperidine (3.34 mL, 39.2 mmol), 4-hydroxybenzaldehyde (1.2 g, 9.82 mmol), $Pd(PPh_3)_4$ (0.136 g, 0.12 mmol), K_2CO_3 (0.54 g, 3.9 mmol), LiCl (0.014 g, 0.32 mmol) in DMF (10 mL) was added to the above pot and irradiated under microwave (180 W, 150 °C) for 45 min. The reaction mixture was cooled to room temperature and filtered through celite and washed with little amount of ethylacetate. The filtrate was poured into water (150 mL), acidified with dil. HCl, (pH = 5–6) and extracted with ethyl acetate (2 × 40 mL). The combined organic layer was washed with water (2 × 15 mL), brine (1 × 10 mL), dried over Na_2SO_4 and vacuum evaporated. The residue was subsequently purified by column chromatography on silica gel (60–120 mesh size) using hexane : ethylacetate (9.4 : 0.6) to give product (**20**).

4-((*E*)-4-((*E*)-4-Hydroxystyryl)styryl)benzene-1,2-diol (20).[32] Green solid (40% yield), mp 293–295 °C, ^1H NMR (CD_3COCD_3 : DMSO-d_6 (7 : 3) 300 MHz), δ (ppm) 7.98 (4H, s), 7.91 (2H, d, J = 8.3 Hz), 7.60 (2H, d, J = 18.1 Hz), 7.54–7.53 (1H, m), 7.51 (2H, d, J = 18.1 Hz), 7.35–7.34 (1H, m), 7.30 (3H, d, J = 8.7 Hz); ^{13}C NMR (75.4 MHz, CD_3COCD_3 : DMSO-d_6 (7 : 3)), δ (ppm) 158.3, 146.5, 146.3, 137.2, 135.5, 129.7, 129.2, 129.0, 128.8, 128.4, 127.0, 126.7, 125.5, 125.4, 119.3, 116.2, 115.7 and 113.9.

The above procedure was also followed for synthesis of other unsymmetrical DSB's **21–26** (Table 1).

Representative procedure for the one pot synthesis of 4,4′,4″-((1*E*,1′*E*,1″*E*)-benzene-1,3,5-triyltris(ethene-2,1-diyl))tris(2,6-dimethoxyphenol) (27, Table 1)

Malonic acid (16.05 g, 154.2 mmol) was taken in a round bottom flask and piperidine (12.75 mL, 128.7 mmol) added gradually. The above mixture was stirred in DMF (30 mL) for 2 min at room temperature. Thereafter, 4-hydroxy-3,5-dimethoxybenzaldehyde (2.36 g, 12.96 mmol), 1,3,5-tribomobenzene (0.75 g, 2.38 mmol), $Pd(PPh_3)_4$ (0.247 g, 0.21 mmol), piperidine (6.37 mL, 63.7 mmol) and LiCl (0.025 g, 0.058 mmol) were added, then reaction mixture allowed to reflux for 16 h. The above mixture was cooled to room temperature and filtered through celite. The filtrate was poured into water (250 mL, acidified with dil. HCl, pH = 5) and extracted with ethyl acetate (3 × 50 mL). The combined organic layer was washed with water (1 × 50 mL), brine (1 × 20 mL), dried over Na_2SO_4 and vacuum evaporated. The residue was subsequently purified by column chromatography on silica gel (60–120 mesh size) using hexane : ethyl acetate (6 : 4) and obtained solid was washed with methanol to provide pure ((*E*,*E*,*E*)-1,3,5-tris(4-hydroxy-3,5-dimethoxy)styrylbenzene) (**27**).

4,4′,4″-((1*E*,1′*E*,1″*E*)-Benzene-1,3,5-triyltris(ethene-2,1-diyl)) tris(2,6-dimethoxyphenol) (27).[9] Yellow solid (30% yield), mp 223–225 °C, ^1H NMR ($CDCl_3$, 300 MHz), δ (ppm) 7.53 (3H, s), 7.17 (3H, d, J = 15.7 Hz), 7.04 (3H, d, J = 15.7 Hz), 6.81 (6H, s), 5.62 (3H, s), 3.98 (18H, s); ^{13}C NMR (75.4 MHz, $CDCl_3$), δ (ppm) 147.4, 138.3, 135.1, 129.4, 129.0, 126.7, 123.4, 103.6 and 56.5. HRMS-ESI: m/z $[M + H]^+$ for $C_{36}H_{36}O_9$, calculated 613.2432; observed 613.2432.

Representative procedure for the synthesis of 3,3″,4,4″,5,5″-hexamethoxy-5′-(3,4,5-trimethoxyphenyl)-1,1′:3′,1″-terphenyl (28, Table 1)

To a stirred mixture of 1,3,5-tribromobenzene (0.95 mmol) in dioxane : water (5 : 1, 10 mL), 3,4,5-trimethoxyphenylboronic acid (3.42 mmol), $Pd(PPh_3)_4$ (0.085 mmol), K_2CO_3 (1.4 mmol) were added and the reaction mixture was irradiated under MW (250 W, 115 °C) for 35 min. The above mixture was cooled to room temperature and was poured into water (250 mL, acidified with dil. HCl, pH = 5) and extracted with ethyl acetate (3 × 50 mL). The combined organic layer was washed with water (1 × 50 mL), brine (1 × 20 mL), dried over Na_2SO_4 and vacuum evaporated. The resulting residue was subsequently purified by column chromatography on silica gel (60–120 mesh size) using hexane : ethyl acetate (9 : 1) to provide pure 1,3,5-tris(3,4,5-trimethoxyphenyl)benzene (**28**).

3,3″,4,4″,5,5″-Hexamethoxy-5′-(3,4,5-trimethoxyphenyl)-1,1′:3′,1″-terphenyl (28). White solid (45% yield), mp 278–280 °C, ^1H NMR ($CDCl_3$, 300 MHz), δ (ppm) 7.68 (3H, s), 6.87 (6H, s), 3.96 (27H, s); ^{13}C NMR (75.4 MHz, $CDCl_3$), δ (ppm) 154.0, 143.1, 138.4, 137.5, 125.7, 105.1, 61.4 and 56.7. HRMS-ESI: m/z $[M + H]^+$ for $C_{33}H_{36}O_9$, calculated 577.2432; observed 577.2456.

Measurement of inhibition of *P. falciparum* growth in culture

In this study, chloroquine sensitive 3D7 and chloroquine resistant Dd2 and INDO strains of *P. falciparum* were cultivated *in vitro* by the method of Trager and Jensen[33] with minor modifications. Cultures were maintained in fresh O+ human erythrocytes at 4% hematocrit in complete medium (RPMI 1640 with 0.2% sodium bicarbonate, 0.5% Albumax, 45 mg L^{-1} hypoxanthine and 50 mg L^{-1} gentamicin) at 37 °C under reduced O_2 (gas mixture 5% O_2, 5% CO_2, and 90% N_2). Stock solutions of chloroquine were prepared in water (Milli Q grade) and test compounds were dissolved in DMSO. All stocks were then diluted with culture medium to achieve the required concentrations (in all cases the final concentration contained 0.4% DMSO, which was found to be non-toxic to the parasite). Drugs and test compounds were then placed in 96-well flat-bottom tissue culture grade plates to yield triplicate wells with drug concentrations ranging from 0 to 100 μM in a final well volume of 100 μL. Chloroquine was used as a positive control in experiments (100 nM with 3D7 and 1000 nM with the chloroquine resistant strains). Parasite culture was synchronized at ring stage with 5% sorbitol. Synchronized culture was aliquoted to a drug containing 96-well plates at 2% hematocrit and 1% parasitemia. After 48 h of incubation under standard culture conditions, plates were harvested and read by the SYBR Green I fluorescence-based method[15] using a 96-well fluorescence plate reader (Victor, Perkin Elmer), with excitation and emission wavelengths at 485 nm and 530 nm, respectively. The fluorescence readings were plotted against drug concentration, and IC_{50} values obtained by visual matching of the drug concentration giving 50% inhibition of growth. In view of the fluorescence basis of the SYBR Green assay, it was important to assess artefacts due to autofluorescence or quenching effects of each test molecule. To measure the auto fluorescence of test molecules, the parasites were treated with 100 μM of all test molecules and incubated for 1 h at 37 °C following which the cultures were lysed by lysis buffer {20 mM Tris; 5 mM EDTA; 0.008% (w/v) saponin; 0.08% (v/v) Triton X, pH 7.5} and read at 485/530 nm (excitation/emission). To determine possible quenching effects, untreated parasite cultures or parasite cultures treated with the test molecules (100 μM) were lysed by 1× SYBR Green I containing lysis buffer and read for their fluorescence values at 485/530 nm (excitation/emission). Comparison of fluorescence counts (+/− test molecule) was used as a measure of quenching or lack of quenching.

Measurement of cytotoxic activity against mammalian cell lines in culture

Animal cell lines (HeLa and fibroblast L929) were used to determine drug toxicity by using MTT assay for mammalian cell viability assay as described by Mosmann[34] using HeLa and fibroblast L929 cells cultured in complete RPMI containing 10% fetal bovine serum, 0.2% sodium bicarbonate and 50 μg mL^{-1} gentamicin. Briefly, cells (10^4 cells per 200 μL per well) were seeded into 96-well flat-bottom tissue-culture plates in complete culture medium. Drug solutions (in all cases the final concentration contained 0.4% DMSO) were added after overnight seeding and incubated for 24 h in a humidified atmosphere at 37 °C and 5% CO_2. DMSO (final concentration 10% v/v) was added as +ve control. An aliquot of a stock solution of 3-(4,5-dimethylthiazol-2-yl)-2,5-diphenyltetrazolium bromide (MTT) (5 mg mL^{-1} in 1× phosphate buffered saline) was added at 20 μL per well, and incubated for another 4 h. After spinning the plate at 1500 rpm for 5 min, supernatant was removed and 100 μL of the stop agent DMSO was added to each well. Formation of formazon, an index of growth, was read at 570 nm and IC_{50} values were determined by analysis of dose–response curves. Selectivity index was calculated as IC_{50} mammalian cell/IC_{50} *Pf* 3D7.

Microscopic evaluation of morphological changes in *P. falciparum*

Morphological changes of *P. falciparum* were monitored by microscopy based Giemsa staining method. Briefly, synchronized ring and trophozoites stage cultures (1% parasitemia, 2% hematocrit) were incubated with IC_{90} of **27** (1.3 μM) and **11** (1.8 μM) for 12, 24, 48 (rings) and 6, 12, 24 h (trophozoites) in wells of 96 well plate. Thin blood smears were prepared from treated and untreated cultures, methanol fixed, stained by Giemsa (Sigma, India) and examined by bright field optical microscopy at 100×.

Detection of DNA fragmentation and chromatin condensation by Hoechst 33342

DNA fragmentation and condensation were detected by Hoechst 33342 (2′-[4-ethoxyphenyl]-5-[4-methyl-1-piperazinyl]-2,5′-bis-1*H* benzimidazoletrihydrochloridetrihydrate, Molecular Probes, USA). Hoechst 33342 stains the condensed chromatin of apoptotic cells far more brightly than is the case with native chromatin of live healthy cells. The assay was performed according to the manufacturer's instruction. Briefly, synchronized ring and trophozoite stage cultures (1% parasitemia and 2% hematocrit) were incubated with IC_{90} of **27** (1.3 μM) and **11** (1.8 μM) for 12, 24, 48 (rings) and 6, 12, 24 h (trophozoites) in wells of 96 well microtiter plate. Cultures were incubated with Hoechst 33342 stain (λ_{max} emission 460 nm) for 20 min at ice temperature. Following transfer of cells to microfuge tubes, the cells were centrifugally washed (200 μL, twice) with PBS and wet mount slides were prepared. The slides were observed by using a fluorescence microscope (Nikon 50i).

Detection of *P. falciparum* mitochondrial trans-membrane potential ($\Delta\Psi_m$)

Changes of *P. falciparum* mitochondrial membrane potential ($\Delta\Psi_m$) were detected by staining with the fluorescent cell-permeable cationic carbocyanine dye JC-1 (5,5′,6,6′-tetrachloro-1,1′,3,3′-tetraethylbenzimidazolylcarbocyanine iodine) (Molecular Probes, USA). JC-1 shows membrane potential dependent transition from a green (λ_{max} emission 525 nm) monomeric form (at low transmembrane potential) to a red (λ_{max} emission 590 nm) aggregated oligomeric form (at higher trans-membrane potential). The assay was performed according to the manufacturer's instructions. Briefly, synchronized ring and trophozoites stage cultures (1% parasitemia and 2% hematocrit) were incubated with IC_{90} of **27** (1.3 μM) and **11** (1.8 μM) for 12, 24, 48 (rings) and 6, 12, 24 h (trophozoites) in wells of 96 well plate. The cultures were incubated with JC-1 dye for 20 min at 37 °C and washed with PBS. Wet mount slides were prepared and observed by using a fluorescence microscope (Nikon 50i) using FITC filter.

Detection of drug induced DNA fragmentation by agarose gel electrophoresis

Drug induced DNA fragmentation was examined by agarose gel electrophoresis. Early trophozoite stage cultures (4% parasitemia) of *Plasmodium falciparum* (Indo) were treated with IC_{90} of **27** (1.3 μM) and **11** (1.8 μM) for 12 and 24 h. CQ (2 μM) was used as positive control. After treatment, the parasites were isolated by the 0.05% saponin treatment procedure, genomic DNA was isolated and samples were analysed by 1% agarose gel electrophoresis method.[35] The gels were photographed using Alpha Imager EC.

Acknowledgements

We graciously acknowledge Department of Science and Technology, New Delhi (Vide Grant No. SR/S1/OC-16/2008). The authors gratefully acknowledge Director(s) of C.S.I.R.-IHBT, I.C.G.E.B., Delhi and C.S.I.R.-C.D.R.I., Lucknow, for their kind cooperation and encouragement. DM and DS thank MR4 who generously provided the chloroquine resistant Dd2 and INDO strains used in the study. Thanks to X. Su and late David Walliker and who deposited these strains with MR4. IHBT Communication No. 2331. DM thanks to ICMR, New Delhi for senior research fellowship. CDRI communication no. 9230.

References

1 A. Trampuz, M. Jereb, I. Muzlovic and R. M. Prabhu, *J. Crit. Care*, 2003, **7**, 315.
2 J. K. Baird, *Antimicrob. Agents Chemother.*, 2011, **55**, 1827.
3 K. A. Roupe, C. M. Remsberg, J. A. Yáñez and N. M. Davies, *Curr. Clin. Pharmacol.*, 2006, **1**, 81.
4 C. Boonlaksiri, W. Oonanant, P. Kongsaeree, P. Kittakoop, M. Tanticharoen and Y. Thebtaranonth, *Phytochemicals*, 2000, **54**, 415.
5 H. Son, M. Chung, S. J. Lee and H. I. Moon, *Parasitol. Res.*, 2007, **101**, 237.
6 M. Jung, W. H. Park, J. C. Jung, E. Lim, Y. Lee, S. Oh and H. I. Moon, *Chem. Biol. Drug Des.*, 2009, **73**, 346.
7 D. P. Flaherty, S. M. Walsh, T. Kiyota, Y. Dong, T. Ikezu and J. L. Vennerstrom, *J. Med. Chem.*, 2007, **50**, 4986.

8 S. R. Byeon, J. H. Lee, Ho. J. Sohn, D. C. Kim, K. J. Shin, K. H. Yoo, I. M. Jung, W. K. Lee and D. J. Kim, *Bioorg. Med. Chem. Lett.*, 2007, **17**, 1466.
9 A. Sharma, N. Sharma, R. Kumar, A. Shard and A. K. Sinha, *Chem. Commun.*, 2010, **46**, 3283.
10 A. K. Sinha, V. Kumar, A. Sharma and A. Sharma, *Tetrahedron*, 2007, **63**, 11070.
11 N. Sharma, A. Sharma, A. Shard, R. Kumar, Saima and A. K. Sinha, *Chem.–Eur. J.*, 2011, **17**, 10350.
12 N. Sharma, D. Mohanakrishnan, A. Shard, A. Sharma, Saima, A. K. Sinha and D. Sahal, *J. Med. Chem.*, 2011, **55**, 297.
13 M. H. Kim and R. B. Cho, *J. Mater. Chem.*, 2009, **19**, 7402.
14 The compound **28** can be considered as an analog of **27** as both these compounds possess similar overall topology and substitution pattern on aryl rings. The replacement of syringol (*i.e.* 4-hydroxy-3,5-dimethoxy) substitution on **27** either by substitution pattern having 4-hydroxy or 4-hydroxy-3-methoxy (*i.e.* (*E*,*E*,*E*)-1,3,5-tris(4-hydroxy)styrylbenzene or (*E*,*E*,*E*)-1,3,5-tris(4-hydroxy-3-methoxy)styryl-benzene) proved unsuccessful due to the formation of several side products.
15 M. Smilkstein, N. Sriwilaijaro, J. X. Kelly, P. Wilairat and M. Riscoe, *Antimicrob. Agents Chemother.*, 2004, **48**, 1803.
16 M. Kimura, H. Narikawa, K. Ohta, K. Hanabusa, H. Shirai and N. Kobayashi, *Chem. Mater.*, 2002, **14**, 2711.
17 S. Xu, Q. Zeng, J. Lu, C. Wang, L. Wan and C. Bai, *Surf. Sci.*, 2003, **538**, L451.
18 A. Jiménez-Ruiz, J. F. Alzate, E. T. MacLeod, C. G. K. Lüder, N. Fasel and H. Hurd, *Parasites Vectors*, 2010, **3**, 104.
19 A. Saraste and K. Pulkki, *Cardiovasc. Res.*, 2000, **45**, 528.
20 J. F. Kerr, *Toxicology*, 2002, **181–182**, 471.
21 S. E. Reece, L. C. Pollitt, N. Colegrave and A. Gardner, *PLoS Pathog.*, 2011, **7**(12), e1002320, DOI: 10.1371/journal.ppat.1002320.
22 A. Debrabant, N. Lee, S. Bertholet, R. Duncan and H. L. Nakhasi, *Int. J. Parasitol.*, 2003, **33**, 257.
23 M. Deponte and K. Becker, *Trends Parasitol.*, 2004, **20**, 165.
24 S. Picot, J. Burnod, V. Bracchi, B. F. Chumpitazi and A. Thomas, *Trans. R. Soc. Trop. Med. Hyg.*, 1997, **91**, 590.
25 B. Meslin, C. Barnadas, V. Boni, C. Latour, F. De Monbrison, K. Kaiser and S. Picot, *J. Infect. Dis.*, 2007, **195**, 1852.
26 B. Meslin, A. H. Beavogui, N. Fasel and S. Picot, *PLoS One*, 2011, **6**, e23867, DOI: 10.1371/journal.pone.0023867.
27 E. MAl-Olayan, G. T. Williams and H. Hurd, *Int. J. Parasitol.*, 2002, **32**, 1133.
28 S. C Arambage, K. M. Grant, I. Pardo, L. Ranford-Cartwright and H. Hurd, *Parasites Vectors*, 2009, **2**, 32.
29 Y. J. Shang, Y. P. Qian, X. D. Liu, F. Dai, X. L. Shang, W. Q. Jia, Q. Liu, J. G. Fang and B. Zhou, *J. Org. Chem.*, 2009, **74**, 5025.
30 M. Yamashita, K. Hirano, T. Satoh and M. Miura, *Chem. Lett.*, 2010, **39**, 68.
31 M. Chalal, D.-F. Vervandier, P. Meunier, H. Cattey and J.-C. Hierso, *Tetrahedron*, 2012, **68**, 3899.
32 D. P. Flaherty, T. Kiyota, Y. Dong, T. Ikezu and J. L. Vennerstrom, *J. Med. Chem.*, 2010, **53**, 7992.
33 W. Trager and J. B. Jensen, *Science*, 1976, **193**, 673.
34 T. J. Mosmann, *Immunol. Methods*, 1983, **65**, 55.
35 K. Moll, A. Kaneko, A. Scherf and M. Wahlgren, *Methods in Malaria Research*, 2013, **6**, 370.

